Current conduction mechanism and electrical break-down in InN grown on GaN

J. Kuzmik, C. Fleury, A. Adikimenakis, D. Gregušová, M. Ťapajna, E. Dobročka, Š. Haščík, M. Kučera, R. Kúdela, M. Androulidaki, D. Pogany, and A. Georgakilas

Citation: Appl. Phys. Lett. **110**, 232103 (2017); doi: 10.1063/1.4985128
View online: http://dx.doi.org/10.1063/1.4985128
View Table of Contents: http://aip.scitation.org/toc/apl/110/23
Published by the American Institute of Physics

Current conduction mechanism and electrical break-down in InN grown on GaN

J. Kuzmik,[1,a)] C. Fleury,[2] A. Adikimenakis,[3] D. Gregušová,[1] M. Ťapajna,[1] E. Dobročka,[1] Š. Haščík,[1] M. Kučera,[1] R. Kúdela,[1] M. Androulidaki,[3] D. Pogany,[2] and A. Georgakilas[3,4]
[1]Institute of Electrical Engineering, Slovak Academy of Sciences, Dúbravska cesta 9, 841 04 Bratislava, Slovakia
[2]Institute for Solid State Electronics, TU Wien, Floragasse 7, A-1040 Vienna, Austria
[3]Microelectronics Research Group (MRG), IESL, FORTH, P.O. Box 1385, 71110 Heraklion, Greece
[4]Department of Physics, University of Crete, 71203 Heraklion, Greece

(Received 16 March 2017; accepted 24 May 2017; published online 8 June 2017)

Current conduction mechanism, including electron mobility, electron drift velocity (v_d) and electrical break-down have been investigated in a 0.5 μm-thick (0001) InN layer grown by molecular-beam epitaxy on a GaN/sapphire template. Electron mobility (μ) of 1040 cm^2/Vs and a free electron concentration (n) of $2.1 \times 10^{18}\,cm^{-3}$ were measured at room temperature with only a limited change down to 20 K, suggesting scattering on dislocations and ionized impurities. Photoluminescence spectra and high-resolution X-ray diffraction correlated with the Hall experiment showing an emission peak at 0.69 eV, a full-width half-maximum of 30 meV, and a dislocation density $N_{dis} \sim 5.6 \times 10^{10}\,cm^{-2}$. Current-voltage ($I$-$V$) characterization was done in a pulsed (10 ns-width) mode on InN resistors prepared by plasma processing and Ohmic contacts evaporation. Resistors with a different channel length ranging from 4 to 15.8 μm obeyed the Ohm law up to an electric field intensity $E_{knee} \sim 22$ kV/cm, when $v_d \geq 2.5 \times 10^5$ m/s. For higher E, I-V curves were nonlinear and evolved with time. Light emission with a photon energy > 0.7 eV has been observed already at modest E_{rad} of ~ 8.3 kV/cm and consequently, a trap-assisted interband tunneling was suggested to play a role. At $E_{knee} \sim 22$ kV/cm, we assumed electron emission from traps, with a positive feed-back for the current enhancement. Catastrophic break-down appeared at $E \sim 25$ kV/cm. Reduction of N_{dis} was suggested to fully exploit InN unique prospects for future high-frequency devices. *Published by AIP Publishing.*
[http://dx.doi.org/10.1063/1.4985128]

InN has been reported as a promising material for ultra-high frequency transistors.[1] This is particularly due to theoretically predicted saturated electron drift velocity (v_d) of ~5–6 × 10^5 m/s at the critical electric field (E_{crit}) of ~23–40 kV/cm.[2–6] This value is significantly higher than v_d ~1 × 10^5 m/s measured in GaN.[7] However, no microwave InN-channel transistor has been demonstrated till now. First experimental attempts on InN-channel transistors were reported either with a 26 nm thick InN grown on AlN,[8] 2–5 nm thick InN grown on zirconia substrates,[9] or 2 nm thick InN on a GaN buffer.[10] In all cases, however, the InN growth was performed with a high strain and inevitable lattice relaxation. Consequently, the electron mobility values (from 20 to 209 cm^2/Vs) indicated significantly degraded InN structural quality, while transistors suffered from an early break-down without the current saturation[8,10] or from a very low current density.[9] Elsewhere, the electron mobility (μ) of 3280 cm^2/Vs has been reported; however, the thickness of the InN layer (d_{InN}) was 5 μm,[11] which is not applicable for the transistor design. Such a high d_{InN} was needed to reduce the dislocation density (N_{dis}) which is typically >$10^{10}\,cm^{-2}$ at the buffer/InN interface.[12–14] However, according to theoretical calculations, N_{dis} as low as $5 \times 10^8\,cm^{-3}$ may be needed to enhance μ.[11] Apart from that, high density defects are located also at the InN surface causing Fermi level pinning in the conduction band, electron accumulation[13,15] and additional μ degradation. To overcome the strain in InN, it was suggested to use InAlN buffer instead of GaN[16] and to use a thin GaN capping on InN to avoid the electron accumulation.[17] Obviously, much effort is needed for microwave InN-channel transistor to become a reality; nevertheless in this paper we test crucial material parameters of the state-of-the art 0.5 μm-thick InN layers: electron mobility, carrier drift velocity and electrical break-down.

(GaN)/InN (0001) sample was grown in a Riber 32p molecular-beam epitaxy (MBE) system equipped with an Oxford HD25 nitrogen RF plasma source.[10,14,18,20] A careful preparation of the growth chamber/vacuum and the source materials was employed to limit the incorporation of unintentional donor impurities, such as oxygen atoms, in the InN layers. The background vacuum of the MBE growth chamber was in the low 10^{-11} Torr range. 300 nm-thick GaN buffer was MBE grown on a commercially available high-resistivity GaN-on-sapphire template, followed by a 0.5 μm-thick InN film grown at 400 °C. An optimized InN growth process was followed according to the results of our previous InN MBE investigations.[14,18,20,21] A stoichiometric[18,21] In/N flux ratio was used to secure a two-dimensional growth mode for InN nucleation on GaN (0001) and subsequent epitaxial growth. The substrate temperature was carefully controlled to avoid any InN decomposition,[14] while providing sufficient diffusion length of the In addatoms on the substrate surface to establish InN growth under the step-flow growth mode.[18,20,21] These conditions result in reduced

a)Electronic mail: Jan.Kuzmik@savba.sk

defect densities and atomically smooth surfaces of the InN layers.[20] Finally, a 5 nm-thick GaN cap layer was grown at 110 °C. The structure was initially characterized by conductivity and Hall Effect measurements ranging from room temperature (RT) down to 20 K, by high-resolution X-ray diffraction (HRXRD), and by photoluminescence (PL). Diffraction analysis was carried out using a Bruker D8 DISCOVER diffractometer equipped with X-ray tube with a rotating Cu anode operating at 12 kW. The density of dislocations with screw (N_{disS}) and edge components (N_{disE}) was evaluated from the X-ray rocking curves.[19,20] Full-width half-maximum (FWHM) values of two symmetric −0002 and 0004 and three skew reflections $-10\bar{1}2$, $11\bar{2}2$, and $10\bar{1}1$ were determined. N_{dis} were calculated as $N_{disS} = \frac{\Gamma_{0°}^2}{1.88 b_s^2}$, $N_{disE} = \frac{\Gamma_{90°}^2}{1.88 b_e^2}$, where Γ_χ are the FWHMs of rocking curves at the inclination angle $\chi = 0°$ and at the extrapolated $\chi = 90°$; $b_s = c = 0.5703$ nm and $b_e = a = 0.3538$ nm are magnitudes of the Burgers vectors of the corresponding dislocations, respectively.[19] PL spectra were recorded at 18 K using the 488 nm line of an Argon ion laser for optical pumping. The PL radiation was dispersed by a quarter-meter monochromator and detected by a liquid-nitrogen-cooled InGaAs photodiode with an extended wavelength range (2250 nm at 77 K).

A special test structure was processed, which comprises InN two-terminal resistors with a length (L) ranging from ∼4 to ∼14 μm and width (w) of ∼4 μm. Mesa regions were defined using an inductive plasma reactive ion etching system by removing 600 nm of the top material. Ohmic contacts were prepared using Ti/Al/Ni/Au. Pulsed *I-V* characteristics of resistors were measured in a four-point configuration using a transmission line pulser with a 10 ns pulse duration (1 ns risetime)[22] to reduce self-heating effects and avoid thermal run-away.[23] *I(t)* and *V(t)* waveforms were recorded by a digital oscilloscope. The pulse repetition frequency was 1 Hz, so the device could cool down to RT before arrival of the next pulse, i.e. there was no heat accumulation. After the each increasing pulse magnitude, the resistor degradation was checked by DC *I-V* measurements. Consequently, v_d was determined as $v_d = I/q\ n\ h\ w$, where h is the InN thickness and n is the free carrier concentration.[7] Light emission was investigated from the polished device backside in a repetitive pulse mode (10 ns duration, 5 ns risetime and 5% duty cycle) using an infrared camera with a wavelength cutoff at ∼1750 nm. The camera frame rate was 50 Hz, so the image was time-averaged approximately over the frame period. The light passed via a 1500 nm long pass edge filter without intensity change, so that the emitted light was in the 1500–1750 nm (0.83–0.71 eV) range. The camera gain has been set to a fixed value, so the measured signal was directly proportional to the light intensity.

Figure 1 shows the Hall Effect free electron concentration and mobility dependence on temperature. At RT, we observed $\mu = 1040\ \text{cm}^2/\text{Vs}$ and $n = 2.1 \times 10^{18}\ \text{cm}^{-3}$, comparing well with the state-of-the-art data for given h.[11,13] We note that because of the InN surface/interface effects, a 3-layer conduction mechanism composing bulk and ∼10 nm thick 2 interfacial layers might be considered by evaluating the Hall Effect measurements.[13,24] Nevertheless, by taking into account $\sim 3 \times 10^{13}\ \text{cm}^{-2}$ and $4 \times 10^{13}\ \text{cm}^{-2}$ electron

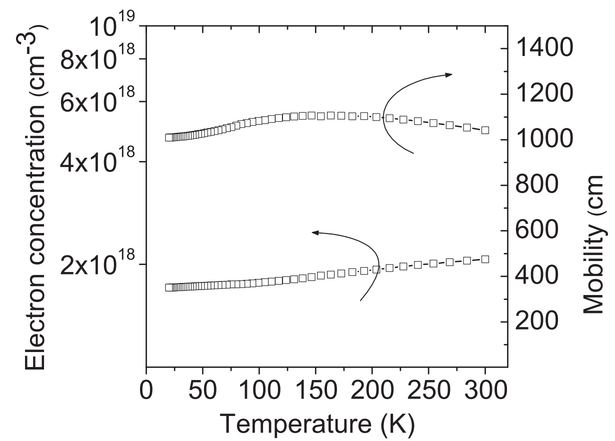

FIG. 1. Directly measured Hall Effect free electron concentration and mobility dependence on temperature in 0.5 μm-thick InN grown on GaN.

accumulation on both sides of the 500-nm thick InN,[24,25] together with degraded mobility by about 75% if compared with a bulk value,[24] at RT, the conduction through thin interfacial layers can be estimated to be only about 15% of the total conduction. The weak temperature dependence of μ indicates scattering on dislocations and ionized impurities, similarly as reported elsewhere.[11,12] This assumption was further proved by extracting N_{dis} from HRXRD rocking curves shown in Fig. 2(a), reaching $7.2 \times 10^8\ \text{cm}^{-2}$ and $5.6 \times 10^{10}\ \text{cm}^{-2}$ for screw and edge dislocations, respectively. It is assumed that desired reduction of N_{dis} will also reduce n which if not under control may increase the InN optical band gap far beyond 1 eV.[26,27] In our case, PL spectra having a peak at 0.69 eV and FWHM of 30 meV prove well controlled n.

The examples of *I(t)* and *V(t)* waveforms for three stress conditions on the InN resistor with $L = 4\ \mu$m are given in Fig. 3(a). Pulsed *I-V* curves, produced by averaging transient data over 2–4 and 6–8 ns time intervals, are given in Fig. 3(b). Several distinguished features can be deduced from the Fig. 3: (i) InN resistor obeys Ohm law up to $V_{knee} = 9.5$ V ($E_{knee} = 24$ kV/cm) when I starts to rise non-linearly, (ii) in the non-linear region I strongly rises with time [see top curves Fig. 3(a)] which leads to a remarkable deviation of *I-V* curves shown in Fig. 3(b), and (iii) pulses are non-destructive up to ∼100 A/mm when a catastrophic breakdown occurs. Striking feature is also a lack of I saturation

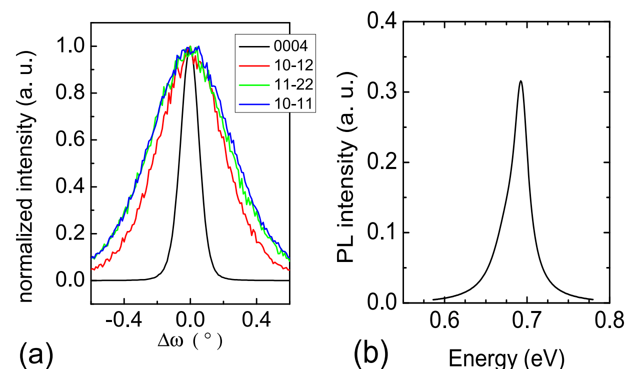

FIG. 2. Crystallographic and optical assessment of InN: (a) HRXRD rocking curves of selected diffractions and (b) PL spectra taken at 18 K.

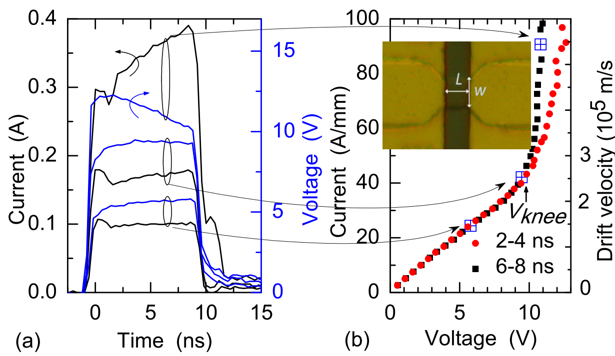

FIG. 3. (a) $I(t)$ and $V(t)$ waveforms and (b) normalized pulsed I-V and v_d–V characteristics of the 4 μm-long InN resistor. The I-V characteristics are obtained by averaging $I(t)$ and $V(t)$ waveforms over 2–4 and 6–8 ns time spans; v_d extraction [right y-axes of Fig. 3(b)] applies only for the linear I-V region. Inset of (b) shows micrograph of the resistor.

which might be a consequence of n increase at $E \geq 24$ kV/cm and related pre-mature break-down at $I \sim 100$ A/mm. Still, in the linear region at V_{knee}, we could extract $v_d \sim 2.5 \times 10^5$ m/s, a promising value for the future device applications. We note up to 15% underestimation of v_d by neglecting conduction through interfacial layers. To push the limits further, in the following, we study mechanism of the transition to the non-linear region by investigating the dependence of E_{knee} on L and temperature (T), and by monitoring the light emission. For the future transistor's speed and power performance, it will be indispensable to demonstrate high v_d and I saturation, e.g., to reach E_{crit} before any non-linear effects appear.

Figure 4 shows similar resistor behavior for all dimensions in respect of the transition to the non-linear I-V region at constant $E_{knee} \sim 22$ kV/cm. Consequently, the mechanism of the transition seems to be driven by the electric field. E_{knee} is found to be independent also on T, as shown in Fig. 5 from RT to 520 K, even though in the linear part I has decreased by about 30% by heating. Here, we point again on Fig. 3(b) where no time dispersion in the linear I-V region proves negligible self-heating, i.e., v_d was not affected by the pulse width. Even more surprising was monitoring the light emission shown in Fig. 6 for $L = 13.8$ μm, with the obvious onset for the InN interband radiative recombination already at E_{rad} ~ 8.3 kV/cm. We note that due to cumulative pulsing, the device degraded before E_{knee}, i.e., we were not able to investigate the light emission in the non-linear region. Nevertheless, in Fig. 7 we show flat and constant optical signal along the resistor at $E \sim 15$ kV/cm. That proves homogeneous distribution of E in the linear I-V region.

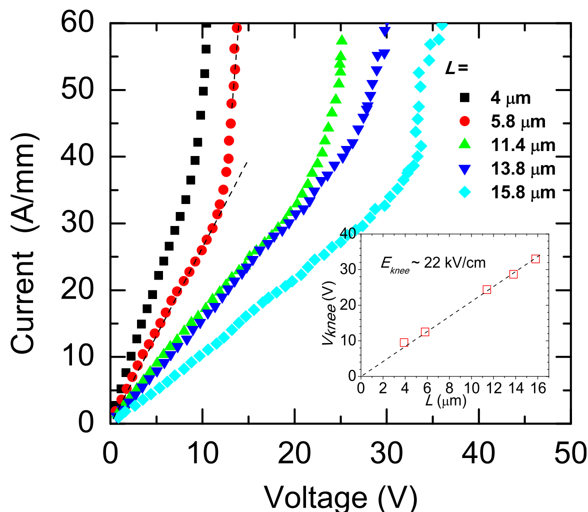

FIG. 4. I-V characteristics of InN resistors with different L. The inset shows V_{knee} dependence on L.

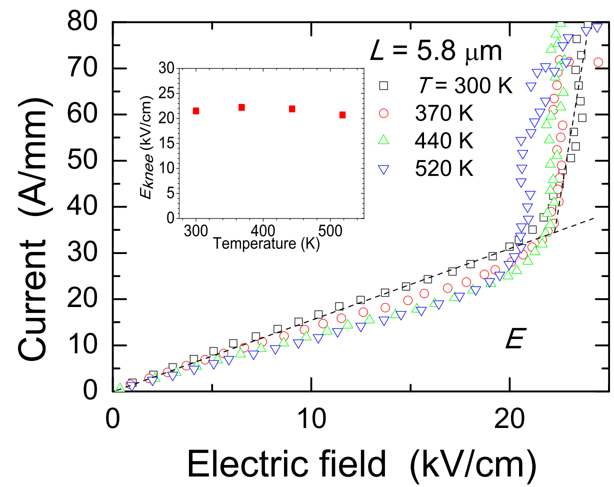

FIG. 5. I-E characteristics of the InN resistor with $L = 5.8$ μm at different T. Inset shows E_{knee} dependence on T.

The assumed increase of n at E_{knee} may be a consequence of interband tunneling which is common for narrow band gap semiconductors, of impact-ionization, or a combination of both.[28,29] However, the impact-ionization seems less likely, taking into account invariant E_{knee} on T, and $\sim$200 kV/cm estimated elsewhere for the avalanche breakdown in a 0.7 eV band gap material.[28] Therefore, the interband tunneling, and in particular, trap assisted tunneling,[30,31] may be a more plausible explanation, starting already at E_{rad} ~ 8.3 kV/cm and triggering the apparent break-down at E_{knee} ~ 22 kV/cm. Nevertheless, it remains to be explained why I rise at E_{knee} coincides with the onset of the transient I-V regime. Here, we believe, a large concentration of N_{dis}-related traps, which is still typical for the state-of-the-art InN layers, play a role. InN is known to have a large number of localized electrons due to the Fermi level pinning in the conduction band.[13,15] Consequently, if E_{knee} represents the onset for the electron emission from traps that may cause I transient with a particular time constant.[31] Moreover, empty

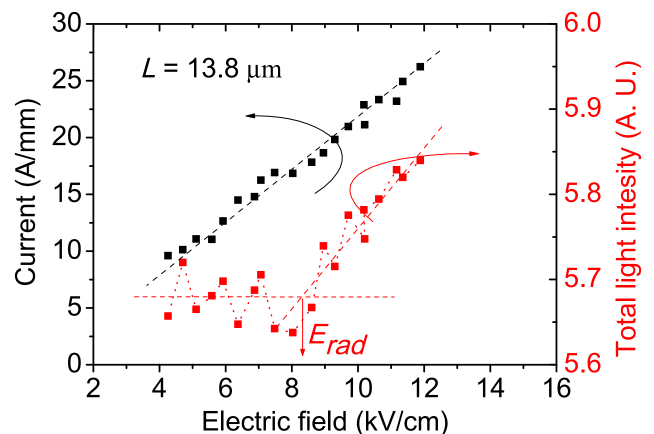

FIG. 6. Current (left axis) and light emission (right axes) dependence on E of the resistor with $L = 13.8$ μm.

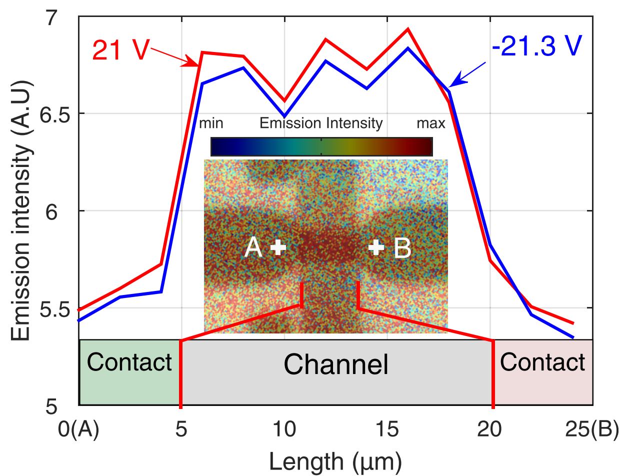

FIG. 7. Averaged light emission along the line AB in the central part of the device (see the inset) at bias ~21 V of both polarities; $L = 13.8\,\mu$m. The inset shows the emission image (color coded) superimposed to backside reflectivity image of the device (shadow background).

states and/or redistributed electric field along the channel[32] may provide a positive feed-back for additional trap-assisted tunneling and/or initiate the avalanche breakdown. Accelerated self-heating can also be considered in this case, as increased n may modify the device thermal resistance by disturbing hot-phonon interactions.[33] Nevertheless, further investigations and physical modeling of InN resistors are needed to fully understand and assign particular mechanisms. We also tested a longer pulse width of 250 ns to enlighten the dynamics of the electron emission however; premature thermal breakdown appeared already before E_{knee} was reached in this case.

In conclusion, by applying 10 ns-long pulses, we studied the electron transport in 0.5 μm-thick InN layer grown on GaN. At RT, structures with the electron mobility of 1040 cm^2/Vs, electron density of 2.1×10^{18} cm^{-3} and dislocation density of 5.6×10^{10} cm^{-2} reached a promising drift velocity of $\sim 2.5 \times 10^5$ m/s at the electric field of ~22 kV/cm, while *I-V* characteristics were still Ohmic. However, a light emission was observed already at $E_{rad} \sim 8.3$ kV/cm which was assigned to intraband trap-assisted tunneling. We suggest a time-dependent electron emission from traps at $E_{knee} \sim 22$ kV/cm providing a positive feed-back for the tunneling and/or triggering the impact ionization. Premature catastrophic break-down appeared at ~25 kV/cm, before reaching the critical field for electron velocity saturation. To increase v_d in InN further and to mitigate non-linear effects, we suggest to reduce the number of N_{dis} by i.e., performing growth with a less strain.[16] Finally, we note that future high-frequency transistors may be designed with the channel length comparable to the electron dead-space having low impact ionization probability.[34] That may also help to prevent pre-mature breakdown.

This project has received funding from the Slovak Agency for R&D, Project No. APVV-15-0031, the Center of Excellence for new technologies in electrical engineering CENTE II, ITMS code 26240120019 (0.4), and from the EU-H2020 research and innovation programme under Grant Agreement No. 654360 NFFA-Europe.

[1]B. E. Foutz, S. K. O'Leary, M. S. Shur, and L. F. Eastman, J. Appl. Phys. **85**, 7727 (1999).
[2]K. T. Tsen, C. Poweleit, D. K. Ferry, H. Lu, and W. J. Schaff, Appl. Phys. Lett. **86**, 222103 (2005).
[3]S. K. O'Leary, B. E. Foutz, M. S. Shur, and L. F. Eastman, Appl. Phys. Lett. **87**, 222103 (2005).
[4]V. M. Polyakov and F. Schwierz, Appl. Phys. Lett. **88**, 032101 (2006).
[5]S. L. Wang, H. X. Liu, B. Gao, J. B. Fan, F. Ma, and Q. W. Kuang, J. Appl. Phys. **111**, 013711 (2012).
[6]W. A. Hadi, P. K. Guram, M. S. Shur, and S. K. O'Leary, J. Appl. Phys. **113**, 113709 (2013).
[7]J. Kuzmik, S. Bychikhin, D. Pogany, C. Gaquiere, and E. Morvan, J. Appl. Phys. **99**, 123720 (2006).
[8]Y.-S. Lin, S.-H. Koa, C.-Y. Chan, S. S. H. Hsu, H.-M. Lee, and S. Gwo, Appl. Phys. Lett. **90**, 142111 (2007).
[9]M. Oseki, K. Okubo, A. Kobayashi, J. Ohta, and H. Fujioka, Sci. Rep. **4**, 3951 (2014).
[10]C. Zervos, A. Adikimenakis, P. Beleniotis, A. Kostoupolos, M. Kayambaki, K. Tsagaraki, G. Konstantinidis, and A. Georgakilas, Appl. Phys. Lett. **108**, 142102 (2016).
[11]X. Wang, S. Liu, N. Ma, L. Feng, G. Chen, F. Xu, N. Tang, S. Huang, K. J. Chen, S. Zhou, and B. Shen, Appl. Phys. Express **5**, 015502 (2012).
[12]K. Wang, Y. Cao, J. Simon, J. Zhang, A. Mintairov, J. Merz, D. Hall, T. Kosel, and D. Jena, Appl. Phys. Lett. **89**, 162110 (2006).
[13]L. F. Piper, T. D. Veal, C. F. McConville, H. Lu, and W. J. Schaff, Appl. Phys. Lett. **88**, 252109 (2006).
[14]E. Dimakis, E. Illiopoulos, K. Tsagaraki, T. Kehagias, P. Komninou, and A. Georgakilas, J. Appl. Phys. **97**, 113520 (2005).
[15]C. G. Van de Walle, J. L. Lyons, and A. Janotti, Phys. Status Solidi A **207**, 1024 (2010).
[16]J. Kuzmik and A. Georgakilas, IEEE Trans. Electron Devices **58**, 720 (2011).
[17]J. Kuzmik, Š. Haščík, M. Kučera, R. Kúdela, E. Dobročka, A. Adikimenakis, M. Micušík, M. Gregor, A. Pleceník, and A. Georgakilas, Appl. Phys. Lett. **107**, 191605 (2015).
[18]E. Dimakis, E. Illiopoulos, K. Tsagaraki, A. Adikimenakis, and A. Georgakilas, Appl. Phys. Lett. **88**, 191918 (2006).
[19]C. S. Gallinat, G. Koblmüller, F. Wu, and J. S. Speck, J. Appl. Phys. **107**, 053517 (2010).
[20]E. Dimakis, J. Z. Domagala, A. Delimitis, P. Komninou, A. Adikimenakis, E. Iliopoulos, and A. Georgakilas, Superlattices Microstruct. **40**, 246 (2006).
[21]E. Dimakis, E. Iliopoulos, M. Kayambaki, K. Tsagaraki, A. Kostopoulos, G. Konstantinidis, and A. Georgakilas, J. Electron. Mater. **36**, 373–378 (2007).
[22]W. Simbürger, D. Johnsson, and M. Stecher, in Proceedings of the ARMMS RF & Microwave Society (2012).
[23]J. Kuzmik, S. Bychikhin, M. Neuburger, A. Dadgar, A. Krost, E. Kohn, and D. Pogany, IEEE Trans. Electron Devices **52**, 1698 (2005).
[24]C. C. Katsidis, A. O. Ajagunna, and A. Georgakilas, J. Appl. Phys. **113**, 073502 (2013).
[25]M. Imura, S. Tsuda, T. Nagata, H. Takeda, M. Liao, A. Yang, Y. Yamashita, H. Yoshikawa, Y. Koide, K. Kobayashi, T. Yamaguchi, M. Kaneko, N. Uematsu, T. Araki, and Y. Nanishi, J. Appl. Phys. **114**, 033505 (2013).
[26]J. Wu, W. Walukiewicz, S. X. Li, R. Armitage, J. C. Ho, E. R. Weber, E. E. Haller, H. Lu, W. J. Schaff, A. Barcz, and R. Jakiela, Appl. Phys. Lett. **84**, 2805 (2004).
[27]M. Tangi, J. Kuyyalil, and S. M. Shivaprasad, J. Appl. Phys. **114**, 153501 (2013).
[28]J. Allam, Jpn. J. Appl. Phys. **36**, 1529 (1997).
[29]S. M. Sze and K. K. Ng, *Physics of Semiconductor Devices* (John Wiley & Sons, Inc., Hoboken, New Jersey, 2007), pp. 102–114.
[30]G. A. M. Hurkx, D. B. M. Klaassen, and M. P. G. Knuvers, IEEE Trans. Electron Devices **39**, 331 (1992).
[31]D. Ielmini, A. S. Spinelli, A. L. Lacaita, A. Martinelli, and G. Ghidini, Solid State Electron. **45**, 1361 (2001).
[32]H. Hasegawa, T. Kitagawa, T. Sawada, and H. Ohno, Electron. Lett. **20**, 561 (1984).
[33]A. Matulionis, J. Liberis, I. Matulioniene, E. Šermukšnis, J. H. Leach, M. Wu, and H. Morkoc, Phys. Status Solidi A **208**, 30 (2011).
[34]S. A. Pimmer, J. P. R. David, R. Grey, and G. J. Rees, IEEE Trans. Electron Devices **47**, 1089 (2000).